Ionic Strength Effect on the Thermal Unfolding of α-Spectrin Peptides†

Denise Lusitani,‡ Nick Menhart,‡ T. A. Keiderling,§ and L. W.-M. Fung*,‡

Department of Chemistry, Loyola University of Chicago, 6525 North Sheridan Road, Chicago, Illinois 60626, and Department of Chemistry, University of Illinois at Chicago, 845 W. Taylor Street, Chicago, Illinois 60607-7061

Received May 15, 1998; Revised Manuscript Received July 31, 1998

ABSTRACT: In previous work, we have shown that the ionic strength-mediated differences found for the hydrodynamic dimensions of the human erythrocyte spectrin are not caused by secondary structural changes, but are caused more probably by subtle changes in tertiary interactions (LaBrake, C. C., Wang, L., Keiderling, T. A., and Fung, L. W.-M. (1993) *Biochemistry 32*, 10296−10302.). The substructure of spectrin has been suggested to be composed largely of triple α-helical bundle structural domains in tandem. In the present study, we used fluorescence and circular dichroism methods to study ionic strength effects on intact spectrin dimers and on recombinant peptides of spectrin domains of different lengths. We observed little ionic strength effect on the thermal unfolding temperature, T_m, values in these systems. However, we found that ionic strength-induced cooperativity in the unfolding processes was similar for the spectrin dimer and for peptides with two or three domains, as measured by entropy changes (ΔS_m). Although single-domain peptides exhibited rather variable ΔS_m values, depending on the specific domain, they showed little salt effects on the ΔS_m values themselves. This suggests that spectrin undergoes subtle ionic strength-induced conformational changes, probably near the interdomain regions of the molecule. These conformational changes may be responsible for the observed hydrodynamic and unfolding properties in intact spectrin under different ionic strength conditions. We suggest that recombinant peptides of various lengths may serve as models for studying the structural flexibility in spectrin.

Human erythrocytes are subjected to various stresses in the circulatory system and are capable of elastic deformation in order to maintain cell integrity. Erythrocytes with abnormal shape and lessened deformability result in early cell death, which leads to symptoms of anemia in patients associated with many hereditary hemolytic anemia diseases. The source of erythrocyte elasticity, although still not clear, has been attributed, in part, to a meshwork of proteins (membrane skeleton) beneath the lipid bilayer and specifically to spectrin, the major protein in the membrane skeleton (*1*).

The basic unit of spectrin is a heterodimer, consisting of two distinct subunits, α-spectrin (280 kDa) and *β*-spectrin (246 kDa), associated laterally in an antiparallel manner (*2*). Spectrin dimers associate to form tetramers (*3*, *4*), which are essential to the formation of the membrane skeleton and thus to the integrity of the cell. Many hereditary hemolytic anemias involve mutations in spectrin (*5*, *6*).

The primary structure of both spectrin subunits was found to consist of many in tandem homologous sequence motifs (*7*−*9*). Each motif is about 106 amino acids in length, with 22 such sequence motifs in α-spectrin and 17 in *β*-spectrin. These homologous sequence motifs have been suggested to fold into similar structural domains, consisting mostly of coiled-coils of triple α-helices (*10*, *11*). Recent X-ray and nuclear magnetic resonance (NMR) studies of spectrin peptides consisting of different single spectrin sequence motifs show that the peptides are indeed folded into triple α-helical bundles (*12*, *13*). Though these highly helical structural domains exhibit independence (*14*), they have also been shown to be interacting substructures that displayed substantial communication between domains (*15*).

Electron microscopy studies have shown that buffer with ionic strength lower than physiological value produces artificially elongated spectrin molecules, either within the membrane skeletal complex (*16*, *17*) or as the independent spectrin tetramer (*18*). The extracted membrane skeleton, and thus spectrin by association, was found to shrink in buffers with increasing ionic strengths (*19*). We have also shown that the Stokes radius of spectrin is larger in low ionic strength buffer than in high ionic strength buffer (*20*). Recent CD and DSC analyses of recombinant peptides of single domain show no ionic strength changes (*14*). Studies of partially extended skeletons in a 2 mM sodium phosphate buffer with 0.05 mM $MgCl_2$ reveal that α- and *β*-spectrin twist around one another, forming a two-start helix with 2-fold rotational symmetry, in which both the pitch and diameter are variable and coupled (*21*). In addition, optical rotary dispersion, calorimetry (*22*), and NMR studies (*23*) of spectrin thermal unfolding detected broader transitions in phosphate buffer (5−15 mM) with no NaCl than in phos-

† This work was supported, in part, by a grant from the National Science Foundation (NSF-MCB9407779 (L.W.M.F.)), a grant from American Heart Association Metropolitan Chicago, a U.S. Department of Education GAANN Fellowship (D.L.), and an American Heart Association Metropolitan Chicago Senior Fellowship (N.M.). Work at UIC was supported in part by the National Institutes of Health (NIH-GM30147 (T.A.K.)).

* To whom correspondence should be addressed. E-mail: lfung@luc.edu.

‡ Loyola University of Chicago.

§ University of Illinois at Chicago.

10.1021/bi9811462 CCC: $15.00
Published on Web 11/06/1998

phate buffer with 100−150 mM NaCl. These studies suggest that intact spectrin molecules in lower ionic strength buffer began to unfold at temperatures lower than those for spectrin in higher ionic strength buffer. However, Fourier transform infrared (FTIR) studies of spectrin dimer at 20 °C in phosphate buffers with different ionic strengths found no evidence of a difference in the fractional secondary structure or in the amide I center frequency which can correlate to α-helical lengths (*20*). Thus it appears that the ionic strength-mediated differences found for the hydrodynamic dimensions and for thermal transition of spectrin are not caused by secondary structural changes, but by subtle changes in tertiary interactions, allowing for a possible rearrangement of the secondary structure elements (*20*).

In this study of spectrin dimer and of recombinant peptides of different lengths, we observed little ionic strength effect on the thermal unfolding temperature values, T_m, as determined by both fluorescence and CD techniques. However, we found that ionic strength-induced cooperativity in the unfolding processes, as measured by entropy changes (ΔS_m), for the spectrin dimer and for peptides with two or three domains was similar. Although single-domain peptides exhibited rather variable ΔS_m values, depending on the specific domain, they showed few ionic strength effects on the ΔS_m values themselves. This suggested that spectrin underwent subtle ionic strength-induced conformational changes, probably near the interdomain regions of the molecule. These conformational changes may be responsible for the observed hydrodynamic and unfolding properties in intact spectrin under different ionic strength conditions. Recombinant peptides of various lengths may serve as models for studying the structural flexibility in spectrin.

EXPERIMENTAL PROCEDURES

Sample Preparation and Characterization. Purification of intact spectrin from human red blood cells (*24*) and of spectrin peptides from *Escherichia coli* (*15*, *25*) was carried out as before. DNA plasmids for six spectrin peptides that corresponded to all possible combinations of the first three full sequence motifs of α-spectrin were constructed, using the phasing determined earlier (*25*). The peptides Spα52−156, Spα157−262, and Spα263−368 consisted of the first, second, and third structural domains, respectively. The peptides Spα52−262 and Spα157−368 consisted of two tandem domains, and Spα52−368 consisted of three tandem domains. These peptides were characterized for solution molecular masses by light scattering and helical contents by FTIR and CD (*15*).

Buffer Systems. Two buffer systems were used for thermal unfolding studies: (1) 5 mM phosphate buffer at pH 7.4 (5P7.4) (This was the low ionic strength buffer.) and (2) 5 mM phosphate buffer with 150 mM NaCl at pH 7.4 (PBS7.4) (This was the high ionic strength buffer.)

Fourier Transform Infrared. FTIR spectra were obtained for these peptides at room temperature in 5P7.4 buffer, using a BIORAD FTS 40 FTIR spectrophotometer (*15*, *20*). Secondary structure analysis was performed on the absorbance spectra of spectrin peptides and spectrin dimers, using the water absorption correction (*26*) and partial least-squares (PLS) analysis methods (*27*), which were also employed in our previous study (*20*). Fourteen spectra of proteins in H_2O buffer, rather than D_2O buffer, with known secondary structures were used as the original training set. These spectra were obtained from Professor M. Pezolet and were input into the PLS QUANT module of the Spectra-Calc program (Galactic Ind., Nashua, NH). A PLS calibration spectrum was calculated using a dimension of 25 and 4 components (ordered α-helix, unordered α-helix, β-sheet, and other, which includes turns and random coil). The values for ordered and unordered α-helix were summed to give the helical contents of samples.

Fluorescence and Circular Dichroism. Thermally induced unfolding of the spectrin peptides and spectrin dimer was monitored by fluorescence spectroscopy, using a Hitachi F-2000 fluorescence spectrophotometer equipped with a thermostated cell holder. A 1 cm path length cuvette was used, with sample stirring, while the temperature was increased continuously at a rate of 1 °C/min. With an excitation wavelength of 278 nm, the emission spectra of samples in either PBS7.4 or 5P7.4 buffer were collected every 2 °C, between 7 and 75 °C. The temperature was measured by a thermal probe inserted into the cuvette. Concentrations for the samples were ∼0.02 mg/mL.

The values of an intensity-weighted mean emission wavelength (λ_{mean}), with λ_{mean} defined as $\sum I_\lambda / \sum I_\lambda \lambda^{-1}$ (*28*, *29*), at each temperature were calculated from fluorescence intensity at each wavelength (I_λ), between 315 and 385 nm (*15*). This parameter is a more suitable measure of unfolding than either simple intensity measurements at a particular wavelength (*30*−*32*) or a ratio of intensities at two wavelengths (*33*). Since λ_{mean} incorporates the information in the whole emission spectra, it is more sensitive to changes in any region of the spectra than results obtained with the other generally used methods mentioned above. Thus λ_{mean} has been used extensively (*34*−*37*).

Thermally induced unfolding of samples either in PBS7.4 or in 5P7.4 was also monitored by circular dichroism (CD) at 222 nm, using a Jasco 710 CD spectrophotometer and a thermostated cell with a 0.1 cm path length. The temperature was increased continuously at a rate of 1 °C/min. Data were collected every 0.5 °C, between 7 and 75 °C. Molar ellipticity at each temperature was determined as before (*15*). Concentrations for samples were ∼ 0.3 mg/mL.

Data Analysis of Thermally Induced Unfolding. Temperature-dependent fluorescence or CD spectral properties, $\phi(T)$, were converted to fraction of unfolding, f_U, at each temperature (T in °C), according to a two-state (native and unfolded states) denaturation model. $\phi(T) = (1 - f_U)\phi_N + (f_U)\phi_U$, where ϕ_N was the value for native state and ϕ_U was the value for unfolded state. From the f_U versus T plots, thermodynamic information was obtained.

Baseline Correction. Spectral intensities obtained in either fluorescence or CD measurements exhibited slight increases upon increasing temperature at temperatures well below or above the transition temperature (For example, see Figure 1, parts A, C, E, and G). These sloping "baselines" were approximated by a linear relationship with temperature (*30*, *38*, *39*). The baseline at temperatures below the transition temperature was represented by

$$\phi_N(T) = \phi_{N,0} + b_N T \quad (1)$$

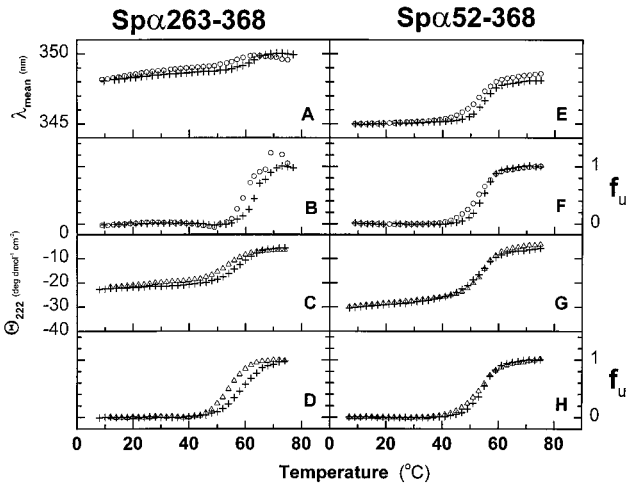

FIGURE 1: Typical thermal denaturation curves of two representative peptides, Spα263−368 (left) and Spα52−368 (right), in 5P7.4 (open symbols) and PBS7.4 (cross) buffers. The intensity weighed mean emission wavelengths, λ_{mean}, of fluorescence measurements as a function of temperature are shown in A and E; the fraction unfolded, f_U, obtained from λ_{mean} as a function of temperature in B (with $\Delta S_{PBS7.4}$ of 1192 J mol^{-1} deg^{-1} and $\Delta S_{5P7.4}$ of 1385 J mol^{-1} deg^{-1}) and F (with $\Delta S_{PBS7.4}$ of 1130 J mol^{-1} deg^{-1} and $\Delta S_{5P7.4}$ of 765 J mol^{-1} deg^{-1}); the molar CD, θ_{222}, from CD measurements as a function of temperature in C and G; and f_U obtained from θ_{222} as a function of temperature in D (with $\Delta S_{PBS7.4}$ of 661 J mol^{-1} deg^{-1} and $\Delta S_{5P7.4}$ of 812 J mol^{-1} deg^{-1}) and H (with $\Delta S_{PBS7.4}$ of 923 J mol^{-1} deg^{-1} and $\Delta S_{5P7.4}$ of 687 J mol^{-1} deg^{-1}).

and at temperatures above transition temperature by

$$\phi_U(T) = \phi_{U,0} + b_U T \quad (2)$$

where $\phi_{N,0}$ and $\phi_{U,0}$ were the spectral properties at a reference temperature (here chosen to be 0 °C for convenience) of state N and state U, respectively, and b_N and b_U were the slope factors, with T in °C. Thus

$$\phi(T) = (1 - f_U)(\phi_{N,0} + b_N T) + f_U(\phi_{U,0} + b_U T) \quad (3)$$

These types of baseline corrections have been widely used (*30*, *40*) and have been rationalized to be due to intrinsic temperature dependence of the spectroscopic properties of the chromophores involved. For example, similar behavior of the intrinsic fluorescence of the indole chromophore of tryptophan in isolated forms has been observed (*41*).

Recently it has been shown that this temperature-dependent baseline may also reflect actual "pretransition" unfolding for local regions of the molecule (*42*−*44*). However, this type of pretransition (local) behavior does not preclude an overall cooperative transition. In this study, we were primarily interested in the overall transition. Thus we treated the sloping signal, whether it originated from the intrinsic fluorescence properties of the chromophore and/or the pretransition unfolding, as baseline and focused on the parameters of the overall transition.

Thermodynamic Parameters of Unfolding. From the relationships of the unfolding reaction equilibrium constant, $K = f_U/(1 - f_U)$ and $K = \exp(-\Delta G/R(T + 273))$, where ΔG is the free-energy change for the unfolding reaction, we obtained

$$f_U/(1 - f_U) = \exp(-\Delta G/R(T + 273)) \quad (4)$$

Table 1: Peptide Molecular Masses (kDa)

peptides	theoretical values[a]	mass spectrometry[b]	light scattering[c] 5P7.4	light scattering[c] PBS7.4
Spα52−156	12.65	12.64	11.9	11.4
Spα157−262	12.24	12.39	9.8	12.4
Spα263−368	12.06	12.21	12.7	12.3
Spα52−262	24.87	24.86	21.5	23.5
Spα157−368	24.28	24.43	26.3	25.9
Spα52−368	36.92	36.92	35.1	34.4

[a] Values calculated from the amino acid sequence of each peptide. [b] Values obtained from time-of-flight matrix-assisted laser desorption ionization mass spectrometry. These values were published (ref *15*) and listed here for comparison. [c] Values were obtained from light scattering measurements. Average values of two runs were listed. The molecular masses were measured either in 5 mM phosphate buffer at pH 7.4 (5P7.4) or in 5 mM phosphate buffer at pH 7.4 with 150 mM NaCl (PBS7.4).

For a linearly temperature-dependent ΔG, where the heat capacity change for the unfolding reaction (ΔC_p) equals 0 (*30*, *39*, *45*), $\Delta G = \Delta H - (T + 273)\Delta S$, where ΔH is the enthalpy change and ΔS is the entropy change for the unfolding reaction. Both ΔH and ΔS are temperature-independent. When $T = T_m$ (melting temperature, with 50% of unfolding), $K = 1$, $\Delta G = 0$, and $\Delta H = (T_m + 273)\Delta S$. Equation 4 was rewritten as

$$f_U/(1 - f_U) = \exp(\Delta S_m(T_m - T)/R(T + 273)) \quad (5)$$

Although in this model ΔS is temperature-independent, we refer to it as ΔS_m to emphasize that we are most concerned with the "melting" process. Though ΔC_p has been shown to be nonzero for most proteins (*39*, *46*−*48*), eq 5 is often used (*30*, *45*) since the relative magnitude of ΔC_p is often not large compared to ΔS. In more rigorous terms,

$$\Delta G = -T_m(\Delta S_g - \Delta C_p) + (\Delta C_p - \Delta S_g)T - \Delta C_p \ln(T/T_m)$$

$$f_U/(1 - f_U) = \exp((T_m(\Delta S_g - \Delta C_p) - T(\Delta S_g - \Delta C_p) - \Delta C_p \ln(T/T_m))/RT) \quad (6)$$

with T in K. ΔS is often referred to as ΔS_g in these equations (entropy change at $\Delta G = 0$). Since at $K = 1$, $\Delta G = 0$, thus $\Delta S_g = \Delta S_m$. The thermal denaturation profiles obtained from either fluorescence or CD measurements were fitted to either eq 5 or eq 6 by the nonlinear regression program provided by Origin (Microcal Software, Inc., Northampton, MA) to give the parameters ΔS_m and T_m from eq 5 and ΔS_g, T_m, and ΔC_p from eq 6. Standard errors of these parameters were also obtained from the program.

Elastase Digestion. Peptide digestion was carried out with elastase from porcine pancreas (Sigma) in 50 mM Tris at pH 8.8 with a peptide to elastase mass ratio of 1:250 (*15*, *25*), and digestion products were analyzed by electrophoresis of 16% gel in the presence of SDS.

RESULTS

Peptide Characterization. All six spectrin peptides were characterized by molecular masses (Table 1) and N-terminal amino acid sequence analysis, similar to those obtained in our earlier studies of these peptides (*15*). In addition, the solution molecular masses determined by light scattering,

Table 2: Structural Properties Derived from FTIR[a]

protein	amide I (cm^{-1})	secondary structural elements[b] % helix	% β-sheet	% other
Spα52−156	1652.0 ± 0.7	45 ± 10	21 ± 7	36 ± 6
Spα157−262	1652.0 ± 0.4	69 ± 3	9 ± 5	21 ± 0
Spα263−368	1652.3 ± 0.2	57 ± 5	14 ± 4	29 ± 2
Spα52−262	1650.8 ± 0.3	69 ± 0	12 ± 2	20 ± 2
Spα157−368	1650.7 ± 0.2	65 ± 4	13 ± 2	23 ± 3
Spα52−368	1650.6 ± 0.1	82 ± 1	6 ± 1	13 ± 1
spectrin dimer	1649.9	67	19	14

[a] All FTIR runs were carried out at room temperature in 5P7.4 buffer. Average values of usually 3 runs are listed with the standard deviation (σ_{n-1}). [b] Partial least-squares analysis (see text) was used to obtain secondary structural element composition.

Table 3: Structural Properties Derived from CD[a]

protein	% helix 5P7.4	PBS7.4
Spα52−156	48 ± 1	52 ± 3
Spα157−262	72 ± 2	75 ± 3
Spα263−368	58 ± 2	61 ± 1
Spα52−262	77 ± 3	75 ± 2
Spα157−368	70 ± 2	72 ± 2
Spα52−368	81 ± 2	79 ± 2
spectrin dimer	53 ± 6	60 ± 10

[a] All CD runs were carried out at room temperature in 5P7.4 or PBS7.4 buffers. Average values of usually 3−5 runs are listed with standard deviation (σ_{n-1}).

in both high ionic strength (PBS7.4) and low ionic strength (5P7.4) buffers (Table 1), indicated that the peptides existed as nonaggregated monomers in these buffers.

Amide I frequency values derived from FTIR measurements provide information on amide C═O hydrogen bond strength along with insight into the conformational characteristics of the peptide chains (*49*). The peak frequencies for the single-domain peptides (Spα52−156, Spα157−262, and Spα263−368) in 5P7.4 buffer at room temperature centered at ∼1652 cm^{-1}, for the peptides with two or three domains (Spα52−262, Spα157−368, and Spα52−368) at ∼1651 cm^{-1}, and for spectrin dimer at ∼1650 cm^{-1}. As expected, the average values of 2−3 runs (Table 2) were similar to those obtained earlier for a single run (*15*). These frequencies are consistent with the expected dominant α-helical conformation of these peptides. The relatively small shifts in the amide I peak positions from 1650 cm^{-1} for the full spectrin dimer to 1651 cm^{-1} for the two- or three-domain peptides, and finally to 1652 cm^{-1} for the single-domain peptides might be thought to be consistent with weaker hydrogen bonding or equivalent to a progressively larger fraction of disordered or shorter segment length helices in the smaller molecular weight peptides. In our earlier FTIR study of the spectrin dimer, we also found that the center frequencies of spectrin dimer treated with SDS upshifted by 3 cm^{-1} and of spectrin treated with NaOH upshifted by 1 cm^{-1} (*20*), indicating less-structured spectrin in SDS or NaOH solution.

The relative content of secondary structural elements obtained from PLS analysis of FTIR spectra showed relatively high helicity (50%−80%) in all peptides in 5P7.4 (Table 2). However, the larger peptides exhibited relatively larger amounts of helices than the smaller peptides, with the helicity in the following order: Spα52−156 < Spα263−368 < Spα157−368 < Spα157−262 ∼ Spα52−262 < Spα52−368. Under the same conditions the spectrin dimer exhibited 67% helical content. It was reassuring that a similar helicity trend was obtained from CD measurements for samples in both 5P7.4 and PBS7.4 (Table 3), with the smaller peptides exhibiting lower helicity than the larger peptides. CD measurements were done at lower protein concentrations than FTIR, eliminating the possibility that FTIR measurements of peptides with higher helicity were stabilized by aggregation at high protein concentrations.

Whether spectrin and spectrin peptides contain any significant fraction of β-sheet is not clear, but is not the focus of this study. The variations of these features (% helix, β-sheet, and others) among the peptides (Table 2) suggested that the secondary structures of these peptides were not identical. It should also be noted that, while X-ray (*12*) and NMR (*13*) data predict about 80% helices (and no β-sheet) for a triple helical structural domain, we and others (*36*) observed lower values for helical contents in various recombinant peptides. The helical contents for Spα52−156 (∼50%) and Spα263−368 (∼60%) were both lower than those found in the peptides of two or three domains (∼70%−80%). However, one of the single-domain peptides, Spa157−262, exhibited higher helical contents (about 70%). Thus we believe that each sequence motif in spectrin can grossly be described as a triple helical bundle, but with varying fine structural features which await further experimental determination.

In general, our results showed that, while the peptides all folded into stable structures with high α-helical contents (FTIR and CD data) and existed as monomers in solution (light scattering data), they each exhibited somewhat different FTIR and CD properties from each other, especially for the single-domain peptides (Spα52−156, Spα157−262, and Spα263−368). The spectrin dimer, while largely composed of the same helical bundle structural domains, also contains other structural features, such as an SH3 domain, two calcium-binding domains in the α-subunit, and an actin-binding domain and a phosphorylation domain in the β-subunit (*1*), and these components make up approximately 10% of spectrin dimer. Thus, we were not surprised to find that the overall helical content for the full spectrin molecule was lower than those in peptides consisting of only two or three domains.

Thermal Unfolding. The thermal unfolding profiles for the spectrin dimer and all six spectrin peptides, in either 5P7.4 or PBS7.4 buffers, from either fluorescence (λ_{mean} vs T; Figure 1, parts A and E, for example) or CD (θ_{222} versus T; Figure 1, parts C and G) measurements, generally showed a single transition, which was more clearly seen by the unfolding fraction plot (f_U vs T; Figure 1, parts B, D, F, and H). Thus, the two-state unfolding model appeared to be valid.

The T_m and ΔS parameters obtained for each system by the two different methods (assuming $\Delta C_p = 0$ (eq 5) or without assuming $\Delta C_p = 0$ (eq 6)) were essentially identical. However, the calculated standard errors of the parameters were quite large when eq 6 was used. For example, for a representative CD spectrum of Spα52−156 in PBS7.4, with eq 5, $\Delta S_m = 526.9 \pm 1.2$ J mol^{-1} deg^{-1} and $T_m = 44.0 \pm 0.1$ °C, and with eq 6, $\Delta S_g = 526.9 \pm 392.9$ J mol^{-1} deg^{-1}

Table 4: Midpoint Unfolding Transition Temperature, T_m (°C)[a]

	fluorescence		circular dichroism	
protein	5P7.4	PBS7.4	5P7.4	PBS7.4
Spα52−156	48 ± 4 (4)	51 ± 2 (4)	45 ± 3 (2)	44 (1)
Spα157−262	58 ± 0 (2)	54 ± 2 (3)	55 ± 2 (2)	53 ± 0 (2)
Spα262−368	59 ± 1 (3)	63 ± 1 (2)	52 ± 2 (3)	57 ± 2 (2)
Spα52−262	51 ± 2 (8)	52 ± 1 (6)	50 ± 1 (3)	50 ± 1 (3)
Spα157−368	61 ± 2 (4)	59 ± 2 (3)	59 ± 1 (3)	57 ± 1 (3)
Spα52−368	52 ± 3 (6)	53 ± 2 (6)	54 ± 1 (3)	54 ± 0 (3)
spectrin dimer	46 ± 0 (4)	47 ± 0 (4)	48 ± 0 (2)	47 (1)

[a] Midpoint unfolding transition temperature values were obtained from curve fitting of fluorescence or CD measurements with eq 5. The number of experimental runs of samples obtained from a single protein preparation for each sample is shown in parentheses following the uncertainty values. We found that samples from different protein preparations exhibited little variation in experimental observations. All uncertainties are the standard deviation of multiple runs (σ_{n-1}).

and $T_m = 44.0 \pm 558.7$ °C and $\Delta C_p = -0.02 \pm 464.24$ J deg^{-1}. The value for ΔC_p obtained from eq 6 (−0.02) was much less than the value for ΔS_g (526.9 J mol^{-1} deg^{-1}). This justified the assumption of $\Delta C_p = 0$ approximation (eq 5). Since ΔG in eq 6 was relatively insensitive to ΔC_p over small temperature ranges when $\Delta C_p \ll \Delta S_g$, the fitting of experimental data to this equation resulted in large uncertainties for all three parameters. We thus concentrated on T_m and ΔS_m parameters obtained from eq 5.

The values of the transition temperature, T_m, of different peptides under high and low ionic strength conditions are summarized in Table 4. The T_m is a common measure of the stability of a protein. For the single-domain peptides, the T_m values varied and appeared to depend on the particular peptide (spectrin domain), on the detection methods (fluorescence or CD), or on the buffer conditions. For example, the value was 63 °C for Spα262−368 and 51 °C for Spα52−156 for samples in PBS7.4, detected by fluorescence. This value of 51 °C for Spα52−156 by fluorescence was compared with the value of 44 °C by CD. The value for Spα157−262, detected by fluorescence, was 58 °C in 5P7.4 and 54 °C in PBS. However, for larger peptides, the T_m values were generally similar in both buffer conditions, and as detected by both methods. For example we obtained T_m values of ∼51 °C for Spα52−262, ∼59 °C for Spα157−368, ∼53 °C for Spα52−368, and ∼47 °C for spectrin dimer.

ΔS may be seen to reflect the cooperativity of the unfolding. High values of ΔS result in steep temperature dependence on ΔG. The larger the value, the sharper the transition. ΔS values obtained from fluorescence and CD measurements were again generally similar, except for Spα263−368 and the spectrin dimer. For example, for Spα52−156 in PBS7.4, the average value was 424 J mol^{-1} deg^{-1} from fluorescence measurements and 524 J mol^{-1} deg^{-1} from CD.

For Spα263−368 and spectrin dimers in either 5P7.4 or PBS7.4, the values from fluorescence were quite different from those from CD (Table 5). For example, for Spα263−368 in PBS7.4, a value of 1214 J mol^{-1} deg^{-1} was obtained by fluorescence methods but 607 J mol^{-1} deg^{-1} by CD methods. The large differences observed between fluorescence and CD for spectrin dimers and Spα263−368 were probably due to the fact that the two methods monitor different unfolding properties. It is likely that systems with certain amounts of intermediate states in unfolding that are detectable by CD but not by fluorescence would show a sharper transition (larger values in ΔS_m) by fluorescence methods. For example, a disruption or unwinding of a particular helical region prior to the final overall unfolding of the helical bundle would be detected by CD, but not necessarily by the fluorescence of a pair of conserved Trp residues. Such pretransition unwinding has been demonstrated in the unfolding of model peptides (*43*, *44*). This contrast of the CD and fluorescence results is very interesting since it may provide some insight into the stability of the helices formed in these peptides. However, this issue is beyond the scope of this paper.

The ΔS_m values of individual peptides in 5P7.4 and in PBS7.4 buffers were quite similar for the peptides with one or two domains, except Spα52−262, indicating little ionic strength effect on the thermal transition in these peptides. However, the three-domain peptide Spα52−368 and the spectrin dimer as well as Spα52−262 exhibited a significantly sharper transition in PBS7.4 than in 5P7.4, suggesting the existence of an ionic strength effect on the thermal transition in these protein systems.

Domain Interaction. We have previously shown that the major elastase digestion product(s) for the two-domain peptide Spα52−262 was a fragment with a gel electrophoresis mass of 14.5 kDa, and for the three-domain peptide Spα52−368 were fragments of 30.5 and 28.3 kDa, which were subsequently digested to a fragment of 14.2 kDa (*15*). Minor components at about 12 and 16 kDa were also observed. In this study we further digested another two-domain peptide, Spα157−368, and found the major digestion product to be 14.3 kDa (Figure 2), similar to that found in Spα52−262. We obtained the sequence of the N-terminal amino acid residues for these digestion products. The first six residues for the 14.5 kDa from Spα52−262 were GSSYHL. The residues GS were from the thrombin digestion site (thrombin was used to cleave fusion proteins), and the remaining sequence matched to residues 52−55 of α-spectrin, indicating that the N-terminal end of Spα52−262 remained after elastase digestion. The first six residues for the 14.3 kDa from Spα157−368 were GSALKF, again with GS corresponding to the thrombin digestion site and ALKF matched to residues 157−160 of α-spectrin, indicating again that the N-terminal end of Spα157−368 remained after digestion.

The first six residues for the intermediate products of Spα52−368 (30.5 and 28.3 kDa fragments) were both GSSYHL (residues 52−55). The first six residues of the subsequent, major product (14.2 kDa) were also GSSYHL, also indicating that the N-terminal end of Spα52−368 remained after elastase digestion.

We used the backbone α carbon coordinates of the X-ray structure (*12*) to generate backbone coordinates for our peptide with three domains (Spα52−368), assuming that the domains were simply connected, with the third helix of the first domain propagated to the first helix of the second domain. Side chains were added to the backbone α carbons, and simple energy minimization was applied to provide a working model for Spα52−368 (Figure 3). This model structure was used to locate the potential digestion sites in a folded structure (Table 6). It appeared that the initial digestion occurred from the C-terminal end, within the loop region connecting helix A to helix B of the last domain of

Table 5: Entropy Change at the Unfolding Midpoint, ΔS_m (J mol^{-1} deg^{-1})[a]

	fluorescence			circular dichroism		
protein	5P7.4	PBS7.4	R^b	5P7.4	PBS7.4	R
Spα52−156	358 ± 100	424 ± 83	1.19	507 ± 91	524	1.03
Spα157−262	890 ± 25	806 ± 33	0.91	981 ± 17	798 ± 83	0.81
Spα263−368	1264 ± 158	1214 ± 33	0.96	657 ±141	607 ± 75	0.92
Spα52−262	615 ± 33	765 ± 42	1.24	615 ± 25	840 ± 33	1.36
Spα157−368	1064 ± 25	1097 ± 67	1.03	1039 ± 67	1048 ± 67	1.01
Spα52−368	757 ± 100	1081 ± 75	1.43	765 ± 42	981 ± 67	1.28
spectrin dimer	1430 ± 125	3658 ±524	2.56	624 ± 17	948	1.52

[a] Values for entropy change of unfolding at 50% unfolding were obtained from curve fitting of fluorescence or CD measurements with eq 5. The number of experimental runs (n) for each value was the same as the corresponding ones in Table 4. All errors were the standard deviation of multiple runs (σ_{n-1}). [b] R (ratio) = mean ΔS_m (PBS7.4)/mean ΔS_m (5P7.4).

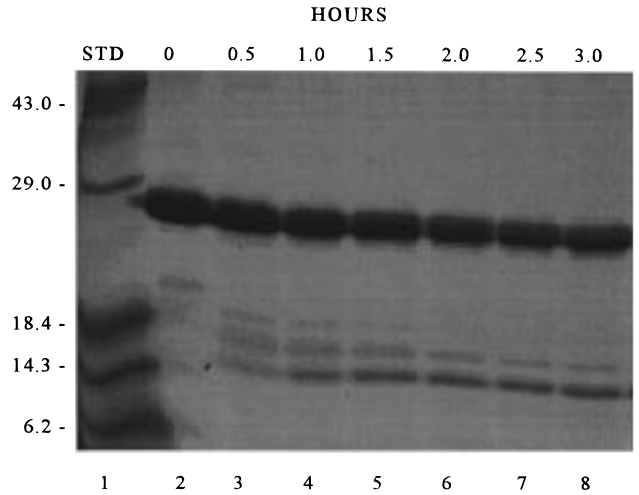

FIGURE 2: SDS−PAGE (16%) of the elastase digestion products of Spα157−368. The first lane contained molecular mass standards. Subsequent lanes (lanes 2−8) contained an aliquot of each digestion reaction ended at various times (0, 0.5, 1, 1.5, 2, 2.5, and 3 h). Intensities of the band for Spα157−368 at 27.2 kDa decreased as a function of elastase digestion time. This band was digested to two major fragments at 16.0 and 14.3 kDa.

the peptide (Table 6, Figure 3) to give a 16 kDa fragment (one complete domain plus a whole helix A) found in samples of both Spα52−262 and Spα157−368 digestion. This fragment was further digested through the middle of helix A of the second domain, producing the 14 kDa fragments (one complete domain plus half of helix A), and finally to the beginning of helix A, producing the 12 kDa fragments (one complete domain). For the peptide with three domains (Spα52−368), the initial digestion in the AB loop produced the 30 kDa fragment. Further digestion from the C-terminal end produced the 16 and 14 kDa fragments. Since this fragment was most resistant to elastase digestion, we suggest that the remaining structural domain gains significant stability, that is, resistance to elastase digestion, from the presence of this short segment of helix A.

DISCUSSION

Spectrin is composed largely of α-helical bundle structural domains, and a single-domain peptide has been shown to be a stable independently folding unit (*14*). Thus, recombinant peptides of individual domains may serve as useful models to study the ionic strength effects in intact spectrin. However, we have shown that peptides with more than one domain are needed to mimic the structural stability of spectrin (*15*). Thus, peptides with two or three domains may be more adequate models for ionic strength effect studies. In this study, we examined three peptides with sequences of three different single domains from spectrin, as well as two peptides with sequences combining two tandem domains, and one peptide with three tandem domains.

While these peptides, among themselves, exhibited somewhat different secondary structural element contents, each peptide individually exhibited little ionic strength effects in the secondary structural element contents. This is in good agreement with our earlier observation on intact spectrin, where we found that the salt-induced contraction and expansion of the erythrocyte skeleton could not be explained by changes in spectrin secondary structure, either in content or in α-helical lengths, and we suggested earlier that it was possible that the helices might change their interactions with each other to favor different sets of molecular interactions under different ionic strength conditions (*20*).

A protein with a high level of cooperativity in thermal unfolding transition remains essentially folded upon temperature increases, until the temperature approaches the transition temperature. Once the temperature reaches the transition value, the unfolding occurs extensively at that temperature to give the unfolded state, resulting in a sharp thermal transition. A ΔG with a steep temperature dependence implies a high value of ΔS_m. A high ratio of ΔS (PBS7.4)/ΔS (5P7.4), the R values in Table 5, reflects a strong ionic strength effect on thermal transition. The R values for the spectrin dimer (2.56 by fluorescence and 1.52 by CD) showed that the spectrin dimer was clearly made more cooperative in thermal unfolding by 150 mM NaCl, although there was no significant change in the T_m value, despite the fact that T_m is usually the most sought after parameter in thermal unfolding experiments.

The broader, less cooperative unfolding of spectrin in 5P7.4 buffer has also been observed in other studies. Broader thermal unfolding transitions have been detected with optical rotary calorimetry (*22*) and with proton NMR (*23*) for spectrin molecules in 5 mM phosphate with no NaCl than in buffer with 100 mM NaCl. It has been suggested that the entropy from the reversible dissociation of weak interactions from interdomain associations drives the elasticity of spectrin, and that these associations could be broken to separate the independently folded domains of spectrin rather than to denature them (*50*). Domain−domain interactions have also been implicated by our earlier studies of these recombinant peptides (*15*).

For the thermal unfolding of spectrin peptides, we observed no systematic stabilization (increase in T_m values)

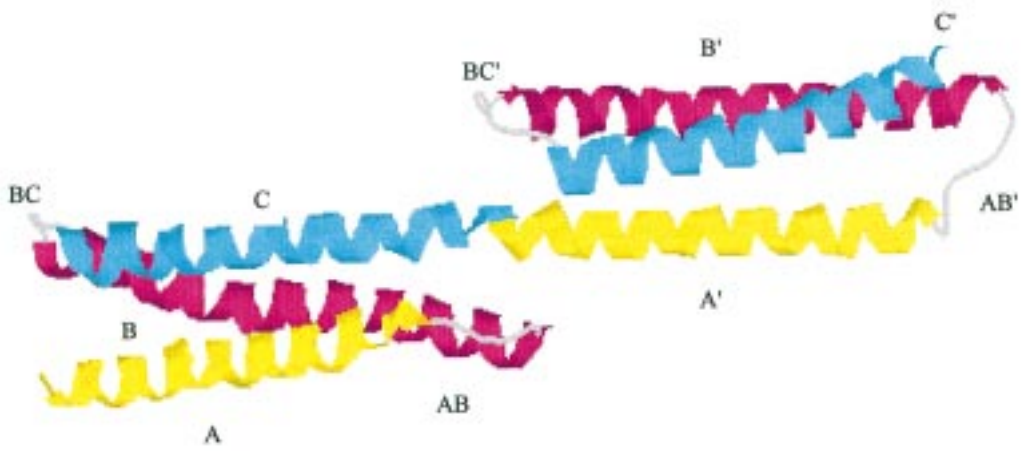

FIGURE 3: Working model of Spα52−262. The model was created by fitting our sequence to the backbone coordinates of the X-ray structure. Energy minimization was applied after the replacement of amino acid side chains. The helices in the triple helical bundles have been designated as helices A, B, and C, starting with the most N-terminal helix. The loops are designated by the regions they link; that is, the loop connecting helix A and helix B is termed the AB loop. The helices and loops of the second domain are designated by the prime symbol. All loops are colored gray, helix A is in yellow, helix B is in red, and helix C is in blue.

Table 6: Characterization of Elastase Digestion Fragments

peptide	mass[a] (kDa)	fragment size[b] (residues)	N-terminal sequence	possible elastase digestion sites (residue number)[c]	digestion sites within triple helical model
Spα52−262 (D1−D2 in tandem)	16.5 (17.116)	135−145		187, 195, or 196	D2 − AB loop[d]
	14.5 (14.859)	115−125	SYHL	170, 171, 174, or 175	D2 − mid helix A
	12.9 (13.485)	105−115		157, 158, or 164	D2 − early helix A
Spα157−368 (D2−D3 in tandem)	16.0 (16.771)	135−145		293, 296−9, or 301−2	D2 − AB loop
	14.3 (14.381)	115−125	ALKF	273, 276−7, or 280	D2 − early helix A
Spα52−368 (D1−D2−D3 in tandem)	30.5 (30.067)	250−260	SYHL	302, 305, or 308−9	D3 − early helix B
	28.3 (28.703)	235−245	SYHL	287, 289, 293, or 296	D3 − AB loop
	16.0 (17.116)	135−145		187, 195, or 196	D2 − AB loop
	14.2 (14.859)	115−125	SYHL	170, 171, 174, or 175	D2 − early helix A

[a] Molecular masses obtained from 16% SDS−PAGE measurements with about 10% uncertainty. The values in parentheses were masses calculated from sequence, using the last possible digestion site as the last residue. For example, for Spα52−262, the value of 17.116 was that of residues 52−196. [b] Fragment sizes (number of amino acid residues) were estimated from molecular masses. [c] Elastase cleaves at the C-terminal side of small nonpolar amino acid residues. We identified residues G, A, V, L, I, and S (ref *55*) in the sequence of α-spectrin as possible digestion sites to give fragments observed by SDS−PAGE. For example, for the 14.5 kDa fragment from Spα52−262, we estimated that the fragment consisted of 115−125 residues. Since the N-terminal residue was residue 52 in α-spectrin, the potential C-terminal residue is around residues 167−177. We examined the α-spectrin sequence around this region and identified residues 170 (I), 171 (L), 174 (I), and 175 (G) as possible elastase digestion sites. [d] See text for the construction of a working model structure for Spα52−368. In this model, the peptide consisted of the first domain, the second domain (D2), and the third domain (D3). Within a domain, helices A, B, and C are arranged in a zigzag manner to form a triple helical bundle, with the AB loop joining helix A and helix B.

or destabilization (decrease in T_m values) of the various peptides by the addition of 150 mM NaCl. For example, Spα263−368 appeared to be stabilized by NaCl by about 4 °C, while Spα157−262 was destabilized by a similar amount. The most and least thermally stable peptides were represented by two of the single-domain peptides (63 °C for Spα263−368 in PBS7.4 with fluorescence methods and 44 °C for Spα52−156 in PBS7.4 by CD methods). There was no trend that we could discern in the distribution of the T_m values over the entire set of peptides. This is in contrast to previous data that has shown that there is a trend whereby the larger peptides are more stable toward solvent denaturation (*15*).

However, a more in depth examination of the ΔS_m data revealed some salient features, though again not so simple. Assuming the unfolded state of all peptides to be similar and to be disordered, we may ascribe increases in the entropy of the unfolding transition to increases in the degree of order of the native state. A native state with a larger number of molecular interactions would remain in an ordered state and exhibit more cooperative unfolding (high ΔS_m), whereas a native state with fewer molecular interactions would remain in a less-ordered structure, and would exhibit a less cooperative unfolding (low ΔS_m). Although most of the peptides showed an increase in ΔS_m in PBS7.4 relative to 5P7.4 (with R values larger than 1), this was not universally true. For example, three of the six peptides (Spα52−156, Spα52−262 and Spα52−368) showed similar salt effects with R(Spα52−368) > R(Spα52−262) > R(Spα52−156). However, two of the peptides showed little effect (Spα263−368 and Spα157−368), while one of them, Spα157−262, in fact showed a salt-mediated decrease in cooperativity with $R <$ 1. Was this weak trend actually evidence for a real ionic strength effect, or simply idiosyncratic differences? The hierarchical nature of the peptides might shed light on this question. These peptides were not simply six randomly chosen spectrin fragments. The Spα52−156, Spα157−262, and Spα52−262 peptides were a subset, with Spα52−156 and Spα157−262 linked in tandem to give Spα52−262, as they are in intact spectrin. This subset is particularly illustrative, since R(Spα52−156) >1 while R(Spα157−262) < 1 and R(Spα52−262) > 1. In fact, R(Spα52−262) was greater than either R(Spα52−156) or R(Spα157−262),

[R(Spα52−156) + R(Spα157−262)]/2, or [R(Spα52−156) × R(Spα157−262)]$^{1/2}$. This indicated that, by linking the two structural domains, we increased the differences between their properties in high and low ionic strength buffers, more than could be accounted for by their properties in the same buffers when isolated. All possible hierarchically linked subsets demonstrated this character, with R(Spα52−368) > [R(Spα52−262) × R(Spα263−368)]$^{1/2}$, or the corresponding arithmetic means, and even R(Spα157−368) > [R(Spα157−262) × R(Spα263−368)]$^{1/2}$. This latter example was again particularly interesting, since both of the constituent single-domain peptides were in fact substantially destabilized, while the two-domain peptide was actually slightly stabilized by high ionic strength. The experimental evidence that the increase in cooperativity was most strongly seen in tandem domain peptides, that the increase became stronger with more domains added, and that spectrin with a very large number of tandem domains showed the largest ionic strength effect of all suggested that this effect was due in some way to the regions joining adjacent domains.

Our elastase digestion data for the two- or three-domain peptides suggested that, in multiple-domain peptides, part of helix A (10−20 residues) of the following domain stabilized the preceding domain of triple α-helical bundles. A recent NMR study of the solution structure of an individual spectrin domain shows that the end of this single domain (the AB loop and the start of helix B) is the most disordered portion of the molecule (*13*). This AB loop is also the most exposed portion of the structure, with the helices at the C-terminus of the peptide not as tightly packed as at the N-terminus. This feature of less helical packing at the C-terminus of a single-domain peptide was also suggested by the X-ray model (*12*). We propose that the disorder in the C-terminus of a single-domain peptide is caused by the lack of the next domain, or simply by the lack of a stretch of helix, to stabilize it. These results support our earlier observation that the single-domain helical bundles are stable units but are not necessarily completely independent domains (*15*).

We suggest that the location of the ionic strength-mediated interactions may be in the interdomain regions. At present, the structural features of the interdomain regions are not known. The general presentation of the peptide structure in Figure 3 may be oversimplified, since it has been suggested that the spectrin subunits are twisted with various pitches and diameters (*21*). Without further information on the specific structure of the interdomain regions, it is difficult to speculate on the mechanism of this ionic strength-induced conformational change. The source of this effect may be complex. The increased stability of proteins with added salt may be due to the increase in the apparent hydrophobic effect due to changes in the solvent structure (*51*), a Hofmeister effect leading to salting out of the nonpolar core. High salt concentration affects water structure, and the orientational correlations of water molecules become more disordered in ionic solutions (*52*). In addition, the dielectric constant decreases as the concentration of salt increases. It has been calculated that there should be a decrease in the dielectric constant of 0.7% for every millimole of KCl per liter (*53*). Based on this, the dielectric constant would decrease by about a factor of 2 in 150 mM NaCl. Thus, addition of salt promotes closer packing of like charges but destabilizes ionic pairing interactions. Except for some specific salt−protein interactions, one of the major effects of electrolytes is the screening of protein−protein electrostatic interactions (*54*). In both precipitation and crystallization, electrostatic shielding of the protein charge is needed for intermolecular interactions. Recently it has been shown that added salt to coiled-coil protein systems can have complex effects on protein stability, involving both stabilizing and destabilizing contributions, with the net effect depending on the nature of the charged residues and the ionic interactions present in the protein (*51*).

In conclusion, we have demonstrated an ionic strength effect in recombinant peptides of spectrin fragments. Since the effect has been intimately linked to a conformational change of intact spectrin, and since a conformational change of spectrin has been linked to its function in maintaining the deformability and elasticity of the erythrocyte membrane (at this time, it is not yet clear that these two conformational changes are the same), it is important to understand this phenomenon. However, this effect has not been observed in recombinant peptides of single domains by DSC (*14*). In this work, we demonstrated that this might be due to the fact that this effect was weak, was somewhat variable in single-domain peptides, and was more pronounced in peptides with more than one domain. In addition, this ionic strength effect was more sophisticated than a simple pleiotropic stabilization, but was rather more easily seen as an increase in cooperativity than as a simple change in secondary structural elements.

REFERENCES

1. Bennett, V., and Gilligan, D. M. (1993) *Annu. Rev. Cell Biol. 9*, 27−66.
2. Speicher, D. W., Morrow, J. S., Knowleds, W. J., and Marchesi, V. T. (1982) *J. Biol. Chem. 257*, 9093−9101.
3. Kam, Z., Josephs, R., Eisenberg, H., and Gratzer, W. B. (1977) *Biochemistry 16*, 5568−5572.
4. Ungewickell, E., and Grazter, W. (1978) *Eur. J. Biochem 88*, 379−385.
5. Marchesi, S. L. (1989) in *Red Blood Cell Membranes: Structure, Function, Clinical Implications* (Agre, P., and Parker, J. C., Eds.) pp 77−110, Marcel Dekker, Inc., New York.
6. Delaunay, J., and Dhermy, D. (1993) *Semin. Hematol. 30*, 21−33.
7. Speicher, D. W., Davis, G., and Marchesi, V. T. (1983) *J. Biol. Chem. 258*, 14938−14947.
8. Sahr, K. E., Laurila, P., Kotula, L., Scarpa, A. L., Coupal, E., Leto, T. L., Linnenbach, A. J, Winkelmann, J. C., Speicher, D. W., Marchesi, V. T., Curtis, P. J., and Forget, B. G. (1990) *J. Biol. Chem. 265*, 4434−4443.
9. Winkelmann, J. C., Costa, F. F., Linzie, B. L., and Forget, B. G. (1990) *J. Biol. Chem. 265*, 20449−54.
10. Speicher, D. W., and Marchesi, V. T. (1984) *Nature 311*, 177−180.
11. Parry, D. A. D., Dixon, T. W., and Cohen, C. (1992) *Biophys. J. 61*, 858−867.
12. Yan, Y., Winograd, E., Viel, A., Cronin, T., Harrison, S. C., and Branton, D. (1993) *Science 262*, 2027−2030.
13. Pascual, J., Pfuhl, M., Walther, D., Saraste, M., and Nilges, M. (1997) *J. Mol. Biol. 273*, 740−751.
14. DeSilva, T. M., Harper, S. L., Kotula, L., Hensley, P., Curtis, P. J., Otvos, L., Jr., and Speicher, D. W. (1997) *Biochemistry 36*, 3991−3997.
15. Menhart, N., Mitchell, T., Lusitani, D., Topouzian, N., and Fung, L. W.-M. (1996) *J. Biol. Chem. 271*, 30410−30416.
16. Byers, T. J., and Branton, D. (1985) *Proc. Natl. Acad. Sci. U.S.A. 82*, 6153−6157.

17. Liu, S.-C., Derick, L. H., and Palek, J. (1987) *J. Cell Biol. 104*, 527−536.
18. Shotton, D. M., Schlunegger, M. O., and Brank, D. (1979) *J. Mol. Biol. 131*, 303−329.
19. Svoboda, K., Schmidt, C. F., Branton, D., and Block, S. M. (1992) *Biophys. J. 63*, 784−793.
20. LaBrake, C. C., Wang, L., Keiderling, T. A., and Fung, L. W.-M. (1993) *Biochemistry 32*, 10296−10302.
21. McGough, A. M., and Josephs, R. (1990) *Proc. Natl. Acad. Sci. U.S.A. 87*, 5208−5212.
22. Ralston, G. B., and Dunbar, J. C. (1979) *Biochim. Biophys. Acta 579*, 20−30.
23. Begg, G. E., Ralston, G. B., and Morris, M. B. (1994) *Biochim. Biophys. Acta 52*, 63−73.
24. Budzynski, D. M., Benight, A. S., LaBrake, C. C., and Fung, L. W.-M. (1992) *Biochemistry 31*, 3653−3660.
25. Lusitani, D. M., Qtaishat, N., LaBrake, C. C., Yu, R. N., Davis, J., Kelley, M. R., and Fung, L. W.-M. (1994) *J. Biol. Chem. 269*, 25955−25958.
26. Dousseau, F., Therrien, M., and Pezolet, M. (1989) *Appl. Spectrosc. 43*, 538−542.
27. Dousseau, F., and Pezolet, M. (1990) *Biochemistry 29*, 8771−8779.
28. Royer, C. A., Mann, C. J., and Matthews, C. R. (1993) *Protein Sci. 2*, 1844−1852.
29. Royer, C. A. (1995) *Methods Mol. Biol. 40*, 65−89.
30. Eftink, M. R. (1994) *Biophys. J. 66*, 482−501.
31. Cai, K., and Schirch, V. (1996) *J. Biol. Chem. 271*, 2987−2994.
32. Gopalan, V., Golbik, R., Schreiber, G., Fersht, A. R., and Altman, S. (1997) *J. Mol. Biol. 267*, 765−769.
33. Steer, B. A., and Merrill, A. R. (1995) *Biochemistry 34*, 7225−7233.
34. Gross, M., Lustig, A., Wallimann, T., and Furter, R. (1995) *Biochemistry 34*, 10350−10357.
35. Zhuang, P., Blackburn, M. N., and Peterson, C. B. (1996) *J. Biol. Chem. 271*, 14323−14332.
36. Pantazatos, D. P., and MacDonald, R. I. (1997) *J. Biol. Chem. 272*, 21052−21059.
37. Sanchez del Pino, M. M., and Fersht, A. R. (1997) *Biochemistry 36*, 5560−5565.
38. Stafford, W. F., III (1985) *Biochemistry 24*, 3314−3321.
39. Shortle, D., Meeker, A. K., and Freire, E. (1988) *Biochemistry 27*, 4761−4768.
40. Lehrer, S. S., and Stafford, W. F., III (1991) *Biochemistry 30*, 5682−5688.
41. Freifelder, D. (1982) *Physical Biochemistry*, pp 537−572 and 691−695, W. H. Freeman and Co., New York.
42. Holtzer, M. E., and Holtzer, A. (1992) *Biopolymers 32*, 1589−1591.
43. Lovett, E. G., d'Avignon, A. D., Holtzer, M. E., Braswell, E. H., Zhu, D., and Holtzer, A. (1996) *Proc. Natl. Acad. Sci. U.S.A. 93*, 1781−1785.
44. Holtzer, M. E., Lovett, E. G., d'Avignon, A. D., and Holtzer, A. (1997) *Biophys. J. 73*, 1031−1041.
45. Hancock, T. J., and Hsu, J. T. (1997) *Magn. Reson. Chem. 35*, 115−123.
46. Sturtevant, J. M. (1977) *Proc. Natl. Acad. Sci. U.S.A. 74*, 2236−2240.
47. Schellman, J. A. (1987) *Annu. Rev. Biophys. Biophys. Chem. 16*, 115−137.
48. Becktel, W. J., and Schellman, J. A. (1987) *Biopolymers 26*, 1859−1877.
49. Jackson, M., and Mantsh, H. H.(1995) *Crit. Rev. Biochem. Mol. Biol. 30*, 95−120.
50. Vertessy, B. G., and Steck, T. L. (1989) *Biophys. J. 55*, 255−262.
51. Kohn, W. D., Kay, C. M., and Hodges, R. S. (1997) *J. Mol. Biol. 267*, 1039−1052.
52. Leberman, R., and Soper, A. K. (1995) *Nature 378*, 364−366.
53. Gabler, R. (1978) in *Electrical Interactions in Molecular Biophysics*, p 100, Academic Press, New York.
54. Beretta, S., Chirico, G., Arosio, D., and Baldini, G. (1997) *Macromolecucles 30*, 7849−7855.
55. Ardelt, W. (1974) *Biochim. Biophys. Acta 341*, 318−326.

BI9811462